Progress In Electromagnetics Research, Vol. 120, 339–353, 2011

EVOLUTION OF BEAM QUALITY AND SHAPE OF HERMITE-GAUSSIAN BEAM IN NON-KOLMOGOROV TURBULENCE

X. Chu*

School of Sciences, Zhejiang Agriculture and Forestry University, Lin'an 311300, China

Abstract—There are many applications of beam quality and beam shape in turbulent atmosphere. Because M^2 factor and kurtosis parameters are often used to descripe beam quality and intensity flatness, the evolution of these two parameters of Hermite-Gaussian beam in turbulent atmosphere have been studied in both theory and numerical calculation. Results show that the spectrum of refractive index fluctuations has a strong effect on these two parameters. For some spectral models, these two parameters are very sensitive to some factors of turbulence. But for other spectral models, the factor is very insensitive to these factors. For example, when the exponent of the spectrum is very small, M^2 factor is very insensitive to the outer scale of turbulence. But when the exponent of the spectrum is very large, the M^2 factor is very insensitive to the inner scale. In addition, we also found that there are many differences between the kurtosis parameters under different conditions. For example, the kurtosis parameters may be very large during propagation. Namely, beam shape may be very sharp under some conditions. When the effects of turbulence is very large or very small, beam shape is very flat.

1. INTRODUCTION

Because of the wide area applications of electromagnetic field [1–5], such as in optical communication [1, 2], laser remote sensing [3, 4] and laser based defense system [5], increasing attention has been paid to the propagation of beam under different conditions in recent years [6–13]. The effects of turbulence on the propagation are one of the important factors. Existing results show that the variations

Received 13 July 2011, Accepted 21 September 2011, Scheduled 22 September 2011

* Corresponding author: Xiuxiang Chu (chuxiuxiang@yahoo.com.cn).

of phase fluctuations [14], angle of arrival fluctuations [15], spreading and direction of beam [16] are different with different power spectrum of refractive index fluctuations. In the past decades, approximately analytical expressions of average intensity for many types of beam with different power spectral models have been derived with the help of zeroth-order approximation (quadratic approximation) [17–23] and first-order approximation [24, 25]. However, it is very difficult to obtain strict analytical expression for average intensity.

Strict analytical expressions of arbitrary moment radius of laser intensity in turbulence can be derived with the help of Wigner transform [26, 27]. From these expressions, not only that many important properties of beam, such as symmetry, beam width, beam quality, beam directionality and the flatness of intensity profile can be precisely studied [28, 29], but also the valid of zeroth- and first-order approximation can be checked.

Hermite-Gaussian beam is a convenient description for the output of lasers whose cavity is not radially symmetric, but rather has a distinction between horizontal and vertical. Its properties both in vacuum and turbulence have been studied extensively due to its wide applications [30–35]. In present paper, our interest is to understand the properties of Hermite-Gaussian beam in non-Kolmogorov turbulence.

2. FORMULATION FOR ARBITRARY MOMENT RADIUS OF HERMITE-GAUSSIAN BEAM

The field amplitude of completely coherent Hermite-Gaussian beam in the plane $z = 0$ is given by [30–35]

$$[U_0(r_0)]_{mn} = B_{mn} H_m\left(\frac{\sqrt{2}}{w_0}x_0\right) H_n\left(\frac{\sqrt{2}}{w_0}y_0\right) \exp\left(-\frac{r_0^2}{w_0^2}\right), \qquad (1)$$

where H_m and H_n are Hermite polynomials, $\mathbf{r}_0 = (x_0, y_0)$ is a two-dimensional vector in the source plane, w_0 is the beam width and $B_{mn} = 1/w_0\sqrt{\pi 2^{m+n-1} m! n!}$ is normalization coefficients. The intensity distribution of such a field has m nodes in the horizontal direction and n nodes in the vertical direction. For $n = m = 0$, Eq. (1) can be simplified to be a Gaussian beam.

Wigner distribution of the cross-spectral density of the field amplitude given in Eq. (1) can be expressed as

$$[h_0(p_0, \theta_0)]_{mn} = \left(\frac{k}{2\pi}\right)^2 \int_{-\infty}^{\infty}\int_{-\infty}^{\infty} \left[U_0\left(p_0 + \frac{q_0}{2}\right)\right]_{mn} \left[U_0^*\left(p_0 - \frac{q_0}{2}\right)\right]_{mn} \exp(-ikq_0 \cdot \theta_0)\, d^2 q_0 \qquad (2)$$

where $\mathbf{p}_0 = (\mathbf{r}_{01} + \mathbf{r}_{02})/2$, $\mathbf{q}_0 = \mathbf{r}_{01} - \mathbf{r}_{02}$, $\boldsymbol{\theta}_0$ are the far-field angular spread and $k = 2\pi/\lambda$ is wave number (λ is wavelength). On substituting from Eqs. (1) into (2), and performing the integration we obtain

$$\begin{aligned}\left[h_0\left(\mathbf{p}_0, \boldsymbol{\theta}_0\right)\right]_{mn} &= (-1)^{m+n}\left(\frac{k}{\pi}\right)^2 \exp\left(-\frac{2p_0^2}{w_0^2} - \frac{1}{2}k^2 w_0^2\theta_0^2\right) \\ &\quad L_m\left(\frac{4p_{0x}^2}{w_0^2} + k^2 w_0^2\theta_{0x}^2\right) L_n\left(\frac{4p_{0y}^2}{w_0^2} + k^2 w_0^2\theta_{0y}^2\right) \quad (3)\end{aligned}$$

where $L_m()$ denotes Laguerre Polynomials, p_{0x}, p_{0y}, θ_{0x} and θ_{0y} are the wave vector component along x-axis and y-axis of $\mathbf{p}_0$ and $\boldsymbol{\theta}_0$, respectively.

From Wigner distribution, arbitrary moment radius of beam can be expressed as

$$\begin{aligned}&\left\langle p_{0x}^{m_1} p_{0y}^{m_2} \theta_{0x}^{n_1} \theta_{0y}^{n_2}\right\rangle \\ &= \frac{1}{P}\int_{-\infty}^{\infty}\int_{-\infty}^{\infty}\int_{-\infty}^{\infty}\int_{-\infty}^{\infty} p_{0x}^{m_1} p_{0y}^{m_2} \theta_{0x}^{n_1} \theta_{0y}^{n_2}\left[h_0\left(\mathbf{p}_0, \boldsymbol{\theta}_0\right)\right]_{mn} d^2\mathbf{p}_0 d^2\boldsymbol{\theta}_0 \quad (4)\end{aligned}$$

where P is the total power of the beam. We substitute Eqs. (3) into (4) to find

$$\begin{aligned}&\left\langle p_{0x}^{m_1} p_{0y}^{m_2} \theta_{0x}^{n_1} \theta_{0y}^{n_2}\right\rangle \\ &= (-1)^{m+n} 2^{\frac{1}{2}(-8-m_1-m_2+n_1+n_2)} (kw_0)^{-n_1-n_2} w_0^{m_1+m_2} \\ &\quad \left[1+(-1)^{m_1}\right]\left[1+(-1)^{m_2}\right]\left[1+(-1)^{n_1}\right]\left[1+(-1)^{n_2}\right] \\ &\quad \times {}_2F_1\left[-m, \tfrac{1}{2}(2+m_1+n_1), 1, 2\right] {}_2F_1\left[-n, \tfrac{1}{2}(2+m_2+n_2), 1, 2\right] \\ &\quad \sec\left(\frac{m_1\pi}{2}\right)\sec\left(\frac{m_2\pi}{2}\right)\frac{\Gamma\left(\frac{1+n_1}{2}\right)\Gamma\left(\frac{1+n_2}{2}\right)}{\Gamma\left(\frac{1-m_1}{2}\right)\Gamma\left(\frac{1-m_2}{2}\right)} \quad (5)\end{aligned}$$

where sec() is the reciprocal of cos(), ${}_2F_1(\cdot)$, $\Gamma(\cdot)$ and ! refer to the hypergeometric function, gamma function and factorial notation, respectively.

With the help of extended Huygens principle and the properties of Dirac delta function, the moment radius of a beam at receiver plane can be expressed as [27]

$$\left\langle p_x^{m_1} p_y^{m_2} \theta_x^{n_1} \theta_y^{n_2}\right\rangle = \left\langle G\left(\mathbf{p}_0, \boldsymbol{\theta}_0\right)\right\rangle \quad (6)$$

where

$$G(\mathbf{p}_0,\boldsymbol{\theta}_0)=\left(\frac{i}{k}\right)^{n_1+n_2+m_1+m_2} z^{m_1+m_2}\int_{-\infty}^{\infty}\int_{-\infty}^{\infty}\int_{-\infty}^{\infty}\int_{-\infty}^{\infty}\delta^{(m_1)}(q_{0x}-q_x)$$
$$\delta^{(m_2)}(q_{0y}-q_y)\,\delta^{(n_1)}(q_x)\,\delta^{(n_2)}(q_y)$$
$$\times\exp\left[\frac{ik}{z}p_0\cdot(q_0-q)+ikq_0\cdot\theta_0-\frac{1}{2}D(q,q_0)\right]d^2qd^2q_0. \quad (7)$$

Here $\delta(\ )$ is the Dirac delta function, z is the propagation distance, $\boldsymbol{\theta}=(\theta_x,\theta_y)$ is the far-field angular spread of a beam at receiver; $p=(p_x,p_y)=(r_1+r_2)/2$ and $q=(q_x,q_y)=r_1-r_2$ where $\mathbf{r}_1$ and $\mathbf{r}_2$ are two-dimensional vectors at receiver. Turbulence structure function $D(q,q_0)$ can be expressed as

$$D(q,q_0)=8\pi^2k^2z\int_0^1 d\xi\int_0^{\infty}\{1-J_0[\kappa|\xi q+(1-\xi)q_0|]\}\Phi(\kappa)\,\kappa d\kappa \quad (8)$$

where J_0 is the Bessel function of zero order, $\Phi(\kappa)$ is the spatial power spectrum of the refractive index fluctuations and κ is the spatial wave number. From Eqs. (5)–(8) arbitrary moment radius of Hermite-Gaussian beam can be derived.

In general, the spatial power spectrum is written as [11, 16]

$$\Phi(\kappa)=A\beta\left(\kappa^2+\kappa_0^2\right)^{-\alpha/2}\exp\left(-\frac{\kappa^2}{\kappa_m^2}\right) \quad (9)$$

where α is the exponent of the spectrum, $A=\sin[(\alpha-3)\pi/2]\,\Gamma(\alpha-1)/\left(4\pi^2\right)$ is a constant that maintains consistency between the index structure function and its power spectrum [9, 11, 16], β is the general refractive index structure constant and has the units of $m^{3-\alpha}$; $K_0=2\pi/L_m$ (L_m is the outer scale of turbulence) and $K_m=2\pi/l_0$ (l_0 is the inner scale of turbulence) [36]. Following Ref. [11], the relation between β and C_n^2 is adopted as $\beta=0.033C_n^2\,(k/z)^{(\alpha-11/3)/2}/A$ in present paper.

3. M^2 FACTOR OF HERMITE-GAUSSIAN BEAM

M^2 factor is a common measure of beam quality of a laser beam. Its value in x direction is defined as

$$M_x^2=2k\left[<x^2><\theta_x^2>-<x\theta_x>^2\right]^{1/2}. \quad (10)$$

If the variable in arbitrary direction is denoted by X (see Fig. 1(a)) and the angle between x axis and X axis is ϕ (See Fig. 1(a)), X and θ_X can be presented as

$$\begin{cases} X=x\cos(\phi)+y\sin(\phi) \\ \theta_X=\theta_x\cos(\phi)+\theta_y\sin(\phi) \end{cases}. \quad (11)$$

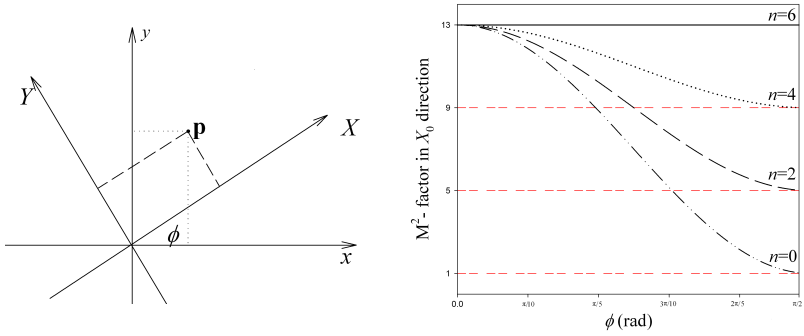

(a) (b)

Figure 1. M^2 factor at source plane or in free space with different ϕ where $m = 6$; (a) Rotation of coordinates in two dimensions; (b) Variation of M^2 factor with ϕ.

From Eqs. (5)–(11) M^2-factor of Hermite-Gaussian beam in X direction at source plane or in free space (in the absence of turbulence) can be expressed as

$$M_{0X}^2 = m + n + (m - n)\cos(2\phi) + 1. \tag{12}$$

Eq. (12) shows that in source plane or in free space, a Hermite-Gaussian beam, related to a TEM_{mn} resonator mode, has an M^2-factor of $(2m + 1)$ in the x direction ($\phi = 0$), and $(2n + 1)$ in the y direction ($\phi = \pi/2$). The variation of M^2-factor in the X direction with ϕ is plotted in Fig. 1(b). Eq. (12) and Fig. 1(b) show that when we set $m > n$, M^2 factor varies within the range $[2n + 1, 2m + 1]$.

From Eqs. (5)–(8), M^2-factor in x direction at z-plane can be derived as

$$M_x^2 = \sqrt{(2m+1)^2 + (2m+1)\left(N_f + \frac{4}{3N_f}\right)G_1 + \frac{4}{3}G_1^2}, \tag{13}$$

where G_1 is the part due to turbulence and can be shown as

$$G_1 = 2\pi^2 k z^2 \int_0^\infty \kappa^3 \Phi(\kappa)\, d\kappa = 0.156\pi^2 N_f^{\frac{\alpha}{2}-\frac{17}{6}} w_0^{\frac{17}{3}-\alpha} r_0^{-5/3} \left[\frac{\kappa_m^{4-\alpha}}{2}\Gamma\left(2 - \frac{\alpha}{2}, \frac{\kappa_0^2}{\kappa_m^2}\right) + \frac{\kappa_0^{4-\alpha}}{2-\alpha}\right]. \tag{14}$$

In Eq. (14), $r_0 = \left(0.423k^2 C_n^2 z\right)^{-3/5}$ is Fried's coherence length, $N_f = kw_0^2/z$ is Fresnel number, and $\Gamma(a, b)$ is the incomplete Gamma function. It should be noted that $\kappa_0 \ll \kappa_m$ is considered in the

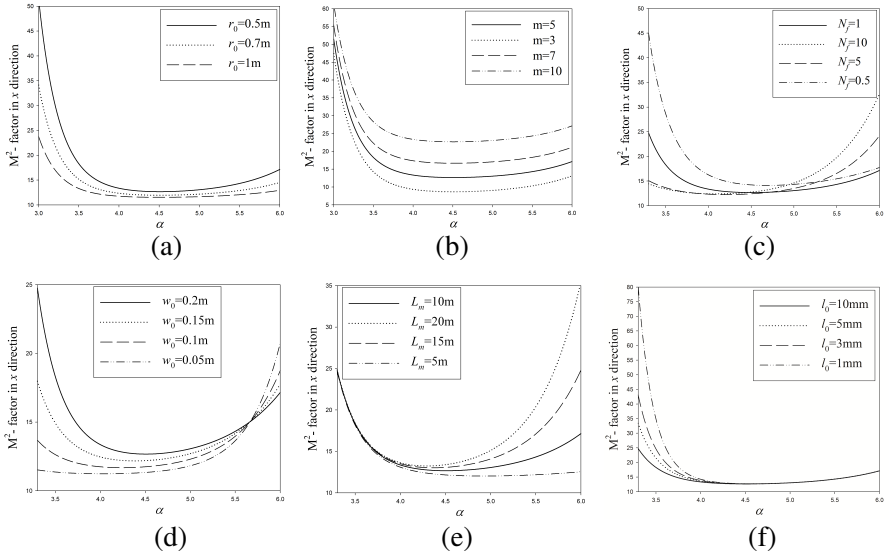

Figure 2. The variation of M^2-factor in x direction with α where (a) $m = 5$, $w_0 = 0.2\,\mathrm{m}$, $N_f = 1$, $L_m = 10\,\mathrm{m}$, $l_0 = 0.01\,\mathrm{m}$; (b) $r_0 = 0.5\,\mathrm{m}$, $w_0 = 0.2\,\mathrm{m}$, $N_f = 1$, $L_m = 10\,\mathrm{m}$, $l_0 = 0.01\,\mathrm{m}$; (c) $m = 5$, $r_0 = 0.5\,\mathrm{m}$, $w_0 = 0.2\,\mathrm{m}$, $L_m = 10\,\mathrm{m}$, $l_0 = 0.01\,\mathrm{m}$; (d) $m = 5$, $r_0 = 0.5\,\mathrm{m}$, $N_f = 1$, $L_m = 10\,\mathrm{m}$, $l_0 = 0.01\,\mathrm{m}$; (e) $m = 5$, $r_0 = 0.5\,\mathrm{m}$, $w_0 = 0.2\,\mathrm{m}$, $N_f = 1$, $l_0 = 0.01\,\mathrm{m}$; (f) $m = 5$, $r_0 = 0.5\,\mathrm{m}$, $w_0 = 0.2\,\mathrm{m}$, $N_f = 1$, $L_m = 10\,\mathrm{m}$.

derivation of Eq. (14), and the term $\kappa_0^{4-\alpha}/(2-\alpha)$ can be neglected if $\alpha < 3$.

The variation of M^2 factor in x direction with α is plotted in Fig. 2. For comparison, these conditions, i.e., $m = 5$, $r_0 = 0.5\,\mathrm{m}$, $w_0 = 0.2\,\mathrm{m}$, $N_f = 1$, $L_m = 10\,\mathrm{m}$ and $l_0 = 0.01\,\mathrm{m}$ are plotted as solid lines in each subfigure. We observe that M^2 factor is larger, or the effect of turbulence on beam quality is larger with smaller or larger α. Fig. 2(a) shows that M^2 factor increases with r_0. The reason is that smaller r_0 means stronger turbulence, it will cause beam quality more degradation. It can be seen from Fig. 2(b) that when α is larger, the variation of M^2 factor for different order Hermite-Gaussian beam agree with each other, and the difference of M^2 between different α becomes small with the decrease of α. Fig. 2(c) shows that there is little difference between $N_f = 10$ and $N_f = 5$ when α is small. However, this difference is quite evident when α is large. The variation of M^2 factor for smaller Fresnel number, i.e., $N_f = 1$ and $N_f = 0.5$, is contrary to that for larger one. The change of M^2 factor with different w_0 is

plotted in Fig. 2(d). It shows that the difference between these w_0 is very large for smaller α. There is a value of α where M^2 factor has the same value for all of the w_0. The effect of outer scale of turbulence on M^2 factor is contrary to that of inner scale (see Figs. 2(e) and 2(f)). For example, the variation of M^2 factor agrees with each other with smaller α. When α is large, M^2 factor has a larger value for larger outer scale, and equal to each other with different inner scales. However, when α is small, the change of M^2 factor with outer scale and inner scale is contrary to the case of large α.

From Eqs. (6)–(8), (10) and (11), we can obtain the formula of M^2-factor in arbitrary direction at z-plane as

$$M_X^2 = \sqrt{\begin{array}{l}[m+n+1+(m-n)\cos(2\phi)]^2 \\ +[m+n+1+(m-n)\cos(2\phi)]\left(N_f+\frac{4}{3N_f}\right)G_1+\frac{4}{3}G_1^2\end{array}} \cdot \quad (15)$$

The comparison between Eqs. (15) and (13) shows that the variation of M^2 factor in X direction is similar to that in x direction. The variation of M^2 factor with ϕ under some conditions is shown in Fig. 3. We can see from Fig. 3 that Hermite-Gaussian beam has different M^2 factor in different direction with different α. The value of M^2 factor along x-axis is the largest one, and decreases with the increase of ϕ (here we set $m > n$). Figs. 3(a) and (b) show that the speed of the decrease with larger r_0 is faster than that with smaller r_0. Namely, we can conclude that the effect of turbulence on beam with larger M^2 factor is smaller than that with smaller M^2 factor. It agrees with the existing result that the turbulence has small effects on partial beam. We also can see from Figs. 3(a) and (b) that when $N_f = 0.5$, M^2 factor becomes smaller for $\alpha = 11/3$, larger for $\alpha = 5.5$ and keeps almost unchanged for $\alpha = 4.5$.

Because Eq. (15) has the same form as Eq. (13), M^2 factor in arbitrary direction can be investigated by using Eq. (13) if we keep m, n and ϕ unchanged. Therefore, further study on the variation of M^2 factor in different direction isn't considered.

3.1. Evolution of the Beam Shape

Kurtosis parameter is defined as $\langle x^4 \rangle / \langle x^2 \rangle^2$, and can be used to describe the sharpness of beam. For example, the top of intensity profile with smaller kurtosis parameters is more flat than that with large kurtosis parameters. From Eqs. (5)–(8) the fourth- and second-

order moment radius can be written as

$$\left\langle x^4 \right\rangle = \frac{3}{16}\left[\left(2m^2+2m+1\right)\left(1+\frac{16}{N_f^4}\right)+\frac{8\left(2m+1\right)^2}{N_f^2} + \frac{8\left(2m+1\right)\left(N_f^2+4\right)}{3N_f^3}G_1+\frac{16G_1^2}{9N_f^2}\right] w_0^4+\frac{3}{10}\pi^2 G_2 \quad (16)$$

and

$$\left\langle x^2 \right\rangle = \left[\left(2m+1\right)\left(\frac{1}{4}+\frac{1}{N_f^2}\right)+\frac{G_1}{3N_f}\right] w_0^2 \quad (17)$$

where

$$G_2 = \frac{z^5}{k^2}\int_0^\infty \kappa^5 \Phi\left(\kappa\right) d\kappa = 0.078 N_f^{\frac{\alpha}{2}-\frac{35}{6}} w_0^{\frac{23}{3}-\alpha} r_0^{-5/3} \left[\frac{\kappa_m^{6-\alpha}}{2}\Gamma\left(3-\frac{\alpha}{2},\frac{\kappa_0^2}{\kappa_m^2}\right)-\frac{\alpha\kappa_0^{6-\alpha}}{\left(\alpha-2\right)\left(\alpha-4\right)}\right]. \quad (18)$$

Because $\kappa_0 \ll \kappa_m$ and α is a positive number, the term $\alpha\kappa_0^{6-\alpha}/\left[\left(\alpha-2\right)\left(\alpha-4\right)\right]$ can be neglected if $\alpha < 5$.

If we set $G_1 = G_2 = 0$ and $N_f \to \infty$, from Eqs. (16) and (17) the kurtosis parameter at source plane can be obtained easily as

$$K_{0X} = \frac{3\left(2m^2+2m+1\right)\cos^4\phi+\left(2m+1\right)\left(2n+1\right)\sin^2 2\phi/2 + \left(2n^2+2n+1\right)\sin^4\phi}{\left[m+n+1+\left(m-n\right)\cos 2\phi\right]^2}. \quad (19)$$

As a comparison, the variation of kurtosis parameter at source plane with m, n and ϕ is shown in Fig. 4.

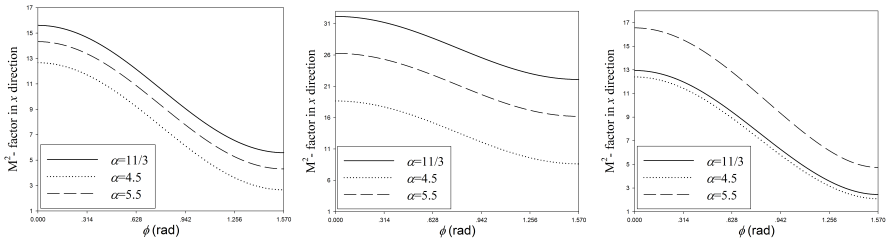

Figure 3. The variation of M^2-factor with ϕ where $m = 5$, $n = 0$, $w_0 = 0.2\,\mathrm{m}$, $L_m = 10\,\mathrm{m}$ and $l_0 = 0.01\,\mathrm{m}$; (a) $r_0 = 0.5\,\mathrm{m}$, $N_f = 1$; (b) $r_0 = 0.2\,\mathrm{m}$, $N_f = 1$ and (c) $r_0 = 0.5\,\mathrm{m}$, $N_f = 0.5$.

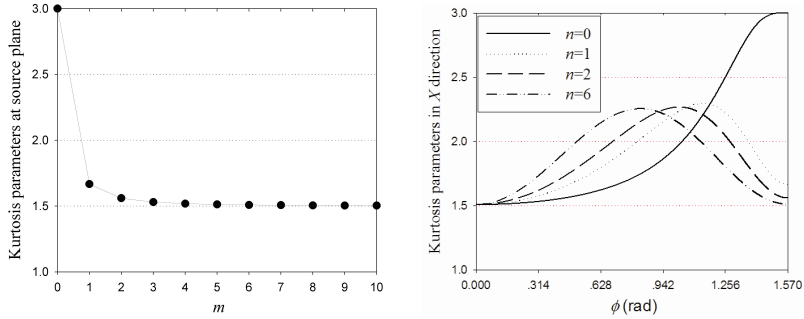

Figure 4. Variation of kurtosis parameters at source plane (a) with m where $\phi = 0$; (b) with ϕ where $m = 6$.

Equation (19) represents that when $m = 0$ the intensity profile in x_0 direction is Gaussian distribution and kurtosis parameter equal 3. As increase m, kurtosis parameter becomes smaller and converges to 1.5. Fig. 4(a) shows that when m is large enough, such as $m \geq 4$, kurtosis parameter keeps almost unchanged. Namely, intensity profile is more flat with large m, and the flatness of beam keeps almost unchanged when $m \geq 4$. It can be seen from Fig. 4(b) that kurtosis parameter increases from 1.5 to 3 when $m = 6$ and $n = 0$. If both of m and n are large, kurtosis parameter increase at beginning, and then decrease. That is to say that intensity profile is more flat along x, and then the flatness becomes worse with the increase of ϕ. When we further increase ϕ the flatness becomes well again.

The kurtosis parameter along x-axis at receiver can also be calculated from Eqs. (16) and (17), as shown in Fig. 5. Comparing Figs. 4 with 5, we can see that the variation of kurtosis parameter at receiver is very different from that at source plane. For example, for very large or very small α, kurtosis parameter at receiver is small. However, the peak value in Fig. 5 is very large and varies with these parameters. If we keep all the other parameters unchanged, the peak value decreases with the increase of m, N_f or l_0 (see Figs. 5(a), (c) and (f)), and increases with the increase of w_0 or r_0 (see Figs. 5(b) and (d)). From Fig. 5(e), we can see that the peak value of kurtosis parameter is independent of L_m. The variations of w_0, r_0, m, N_f or l_0 not only affect the peak value, but also affect the corresponding α. Besides these, we also find that the effect of outer scale on kurtosis parameter is different from that of inner scale. The difference of kurtosis parameter with different L_m is evident only when α is very large. However, the

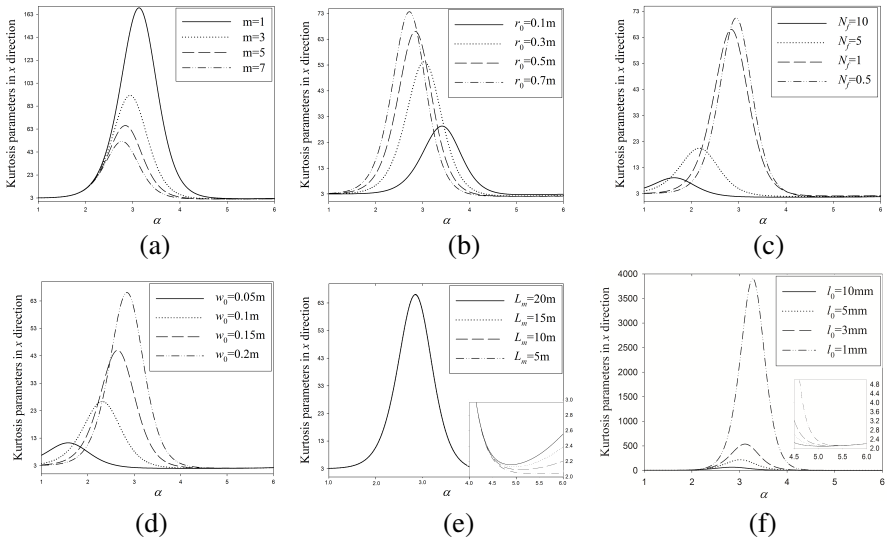

Figure 5. Variation of kurtosis parameter along x-axis at receiver where (a) $r_0 = 0.5\,\mathrm{m}$, $w_0 = 0.2\,\mathrm{m}$, $N_f = 1$, $L_m = 10\,\mathrm{m}$, $l_0 = 0.01\,\mathrm{m}$; (b) $m = 5$, $w_0 = 0.2\,\mathrm{m}$, $N_f = 1$, $L_m = 10\,\mathrm{m}$, $l_0 = 0.01\,\mathrm{m}$; (c) $m = 5$, $r_0 = 0.5\,\mathrm{m}$, $w_0 = 0.2\,\mathrm{m}$, $L_m = 10\,\mathrm{m}$, $l_0 = 0.01\,\mathrm{m}$; (d) $m = 5$, $r_0 = 0.5\,\mathrm{m}$, $N_f = 1$, $L_m = 10\,\mathrm{m}$, $l_0 = 0.01\,\mathrm{m}$; (e) $m = 5$, $r_0 = 0.5\,\mathrm{m}$, $w_0 = 0.2\,\mathrm{m}$, $N_f = 1$, $l_0 = 0.01\,\mathrm{m}$; (f) $m = 5$, $r_0 = 0.5\,\mathrm{m}$, $w_0 = 0.2\,\mathrm{m}$, $N_f = 1$, $L_m = 10\,\mathrm{m}$.

difference of kurtosis parameter with different l_0 is quite evident when α is not large enough. With the increase of α, this difference disappears gradually.

Because $\langle x^{m_1} y^{n_1} \rangle = 0$ if $m_1 + n_1$ is odd, and

$$\left\langle x^2 y^2 \right\rangle = \left[(2m+1)(2n+1)\left(\frac{1}{4}+\frac{1}{N_f^2}\right)^2 + (m+n+1)\left(\frac{2}{3N_f^3}+\frac{1}{6N_f}\right)G_1 + \frac{G_1^2}{9N_f^2}\right] w_0^4 + \frac{1}{10}\pi^2 G_2 \tag{20}$$

from Eqs. (11), (16) and (17) the kurtosis parameter in arbitrary direction can be calculated, as shown in Fig. 6.

It can be seen from Figs. 6(a), (b) and (c) that when n is smaller than m, kurtosis parameter increases slowly at beginning; after this, the kurtosis parameter increases quickly. When ϕ approach to $\pi/2$, the increase becomes slow again. If the kurtosis parameters along x axis

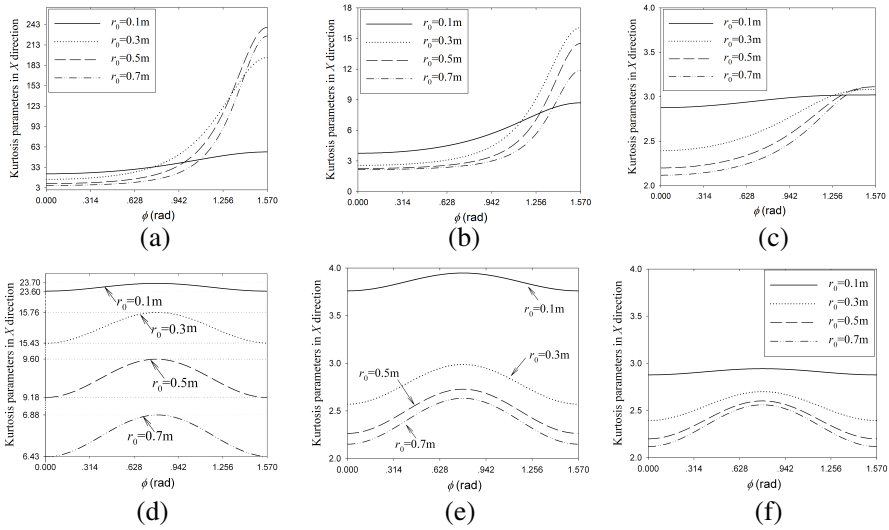

Figure 6. The kurtosis parameter at receiver in arbitrary direction where $m = 5$, $w_0 = 0.2\,\mathrm{m}$, $N_f = 1$, $L_m = 10\,\mathrm{m}$ and $l_0 = 0.01\,\mathrm{m}$; (a) $n = 0$, $\alpha = 11/3$; (b) $n = 0$, $\alpha = 4.5$; (c) $n = 0$, $\alpha = 5.5$; (d) $n = 5$, $\alpha = 11/3$, (e) $n = 5$, $\alpha = 4.5$; (f) $n = 5$, $\alpha = 5.5$.

and y axis are equal (see Figs. 6(d), (e) and (f)), the kurtosis parameter corresponding to $\phi = \pi/4$ is the maximum value. The difference of kurtosis parameter between $y = x$ and x axis becomes small with the decrease of r_0. It means that strong turbulence will make beam smooth in every direction. Because the evolution of kurtosis parameter with ϕ is determined by the difference between the kurtosis parameter along x axis and y axis, and the difference can be found in Fig. 5, the effects of the other parameters, such as w_0, N_f, L_m and l_0, on the evolution of kurtosis parameter aren't taken into account.

4. CONCLUSION

With the help of Wigner transform, strict analytical expression of analytical arbitrary moment radius for Hermite-Gaussian beam in turbulent atmosphere has been derived. Based on the formula the evolution of M^2 factor and kurtosis parameter is investigated in detail. The specific conclusions derived from the study can be listed as follows:

(1) M^2 factor is larger, i.e., beam quality is worse with smaller or larger α when the other parameters keep unchanged.

(2) When we decrease Fresnel number, or increase w_0, M^2 factor

increases for larger α and decreases for smaller α.

(3) M^2 factor is independent of outer scale when α is smaller, and on inner scale when α is larger.

(4) Kurtosis parameter will be of great change when changing the conditions. The peak value of kurtosis parameter and corresponding α varies with the change of parameters. It means that beam shape can be very sharp by selecting suitable parameters.

(5) When α is very smaller, the variation of outer scale cannot affect the kurtosis parameter. However, when α is very larger, the difference of the kurtosis parameter due to the variation of outer scale become larger. Inner scales have contrary effects on the kurtosis parameter for very larger or smaller α.

(6) When α is very larger or smaller, the effects of m, r_0, N_f and w_0 on kurtosis parameter become very small.

REFERENCES

1. Vilnrotter, V., "Optical array receiver for communication through atmospheric turbulence," *J. Lightwave Tech.*, Vol. 23, 1664–1675, 2005.
2. Lee, H.-S., "A photon modeling method for the characterization of indoor optical wireless communication," *Progress In Electromagnetics Research*, Vol. 92, 121–136, 2009.
3. Extermann, J., P. Béjot, L. Bonacina, P. Billaud, J. Kasparian, and J. P. Wolf, "Effects of atmospheric turbulence on remote optimal control experiments," *Appl. Phys. Lett.*, Vol. 92, 041103-5, 2008.
4. Meng, Y. S., Y. H. Lee, and B. C. Ng, "Further study of rainfall effect on VHF forested radio-wave propagation with four-layered model," *Progress In Electromagnetics Research*, Vol. 99, 149–161, 2009.
5. Duff, E. A. and D. C. Washburn, "The magic of relay mirrors," *Proc. SPIE*, Vol. 5413, 137–144, 2004.
6. Li, Y. and H. Ling, "Numerical modeling and mechanism analysis of VHF wave propagation in forested environments using the equivalent slab model," *Progress In Electromagnetics Research*, Vol. 91, 17–34, 2009.
7. Golbraikh, E., H. Branover, N. S. Kopeika, and A. Zilberman, "Non-Kolmogorov atmospheric turbulence and optical signal propagation," *Nonlinear Proc. in Geoph.*, Vol. 13, 297–301, 2006.
8. Hasar, U. C., G. Akkaya, M. Aktan, C. Gozu, and A. C. Aydin, "Water-to-cement ratio prediction using anns from non-

destructive and contactless microwave measurements," *Progress In Electromagnetics Research*, Vol. 94, 311–325, 2009.

9. Toselli, I., L. C. Andrews, R. L. Phillips, and V. Ferrero, "Free-space optical system performance for laser beam propagation through non-Kolmogorov turbulence," *Opt. Eng.*, Vol. 47, No. 2, 026003-9, 2008.
10. Alexopoulos, A., "Effect of atmospheric propagation in RCS predictions," *Progress In Electromagnetics Research*, Vol. 101, 277–290, 2010.
11. Zilberman, A., E. Golbraikh, and N. S. Kopeika, "Propagation of electromagnetic waves in Kolmogorov and non-Kolmogorov atmospheric turbulence: three-layer altitude model," *Appl. Opt.*, Vol. 47, 6385–6391, 2008.
12. Gay-Fernandez, J. A., M. Garcia Sanchez, I. Cuinas, A. V. Alejos, J. G. Sanchez, and J. L. Miranda-Sierra, "Propagation analysis and deployment of a wireless sensor network in a forest," *Progress In Electromagnetics Research*, Vol. 106, 121–145, 2010.
13. Pavelyev, A. G., Y.-A. Liou, J. Wickert, K. Zhang, C.-S. Wang, and Y. Kuleshov, "Analytical model of electromagnetic waves propagation and location of inclined plasma layers using occultation data," *Progress In Electromagnetics Research*, Vol. 106, 177–202, 2010.
14. Rao, C., W. Jiang, and N. Ling, "Spatial and temporal characterization of phase fluctuations in non-Kolmogorov atmospheric turbulence," *J. Mod. Opt.*, Vol. 47, 1111–1126, 2000.
15. Toselli, I., L. C. Andrews, R. L. Phillips, and V. Ferrero, "Angle of arrival fluctuations for free space laser beam propagation through non Kolmogorov turbulence," *Proc. SPIE 65510E*, 1–12, 2007.
16. Wu, G., H. Guo, S. Yu, and B. Luo, "Spreading and direction of Gaussian–Schell model beam through a non-Kolmogorov turbulence," *Opt. Lett.*, Vol. 35, 715, 2010.
17. Cai, Y. and S. He, "Propagation of a partially coherent twisted anisotropic Gaussian Schell-model beam in a turbulent atmosphere," *Appl. Phys. Lett.*, Vol. 89, 041117-9, 2006.
18. Eyyuboğlu, H. T. and Y. Baykal, "Average intensity and spreading of cosh-Gaussian laser beams in the turbulent atmosphere," *Applied Optics*, Vol. 44, No. 6, 976–983, 2005.
19. Zhang, E., X. Ji, and B. Lu, "Changes in the spectrum of diffracted pulsed cosh-Gaussian beams propagating through atmospheric turbulence," *Journal of Optics A: Pure and Applied Optics*, Vol. 9, 951–957, 2007.

20. Zhu, Y. and D. Zhao, "Propagation of a stochastic electromagnetic Gaussian Schell-model beam through an optical system in turbulent atmosphere," *Applied Physics B: Lasers and Optics*, Vol. 96, 155–160, 2009.
21. Wang, F., Y. Cai, H. T. Eyyuboglu, and Y. K. Baykal, "Average intensity and spreading of partially coherent standard and elegant laguerre-gaussian beams in turbulent atmosphere," *Progress In Electromagnetics Research*, Vol. 103, 33–56, 2010.
22. Golbraikh, E. and S. S. Moiseev, "Different spectra formation in the presence of helical transfer," *Phys. Lett. A*, Vol. 305, 173–175, 2002.
23. Wei, H. Y., Z. S. Wu, and Q. Ma, "Log-amplitude variance of laser beam propagation on the slant path through the turbulent atmosphere," *Progress In Electromagnetics Research*, Vol. 108, 277–291, 2010.
24. Wandzura, S. M., "Systematic corrections to quadratic approximations for power-law structure functions: The delta expansion," *J. Opt. Soc. Am.*, Vol. 71, 321–326, 1981.
25. Chu, X. and G. Zhou, "First-order approximation in studying beam spreading of cosh-Gaussian and cos-Gaussian beam in Kolmogorov turbulence," *Appl. Phy. B*, Vol. 101, 381–392, 2010.
26. Salem, M., T. Shirai, A. Dogariu, and E. Wolf, "Long-distance propagation of partially coherent beams through atmospheric turbulence," *Optics Commun.*, Vol. 216, 261–265, 2003.
27. Dan, Y. and B. Zhang, "Second moments of partially coherent beams in atmospheric turbulence," *Opt. Lett.*, Vol. 34, 563–565, 2009.
28. Zhou, P., Y. Ma, X. Wang, H. Zhao, and Z. Liu, "Average spreading of a Gaussian beam array in non-Kolmogorov turbulence," *Opt. Lett.*, Vol. 35, 1043–1045, 2010.
29. Wu, G., T. Zhao, J. Ren, J. Zhang, X. Zhang, and W. Li, "Beam propagation factor of partially coherent Hermite-Gaussian beams through non-Kolmogorov turbulence," *Opt. & Laser Tech.*, Apr. 11, 2011.
30. Huang, Y., G. Zhao, Z. Duan, D. He, Z. Gao, and F. Wang, "Spreading and M^2-factor of elegant Hermite-Gaussian beams through non-Kolmogorov turbulence," *J. Mod. Opt.*, May 6, 2011.
31. Wu, G., B. Luo, S. Yuc, A. Dang, T. Zhao, and H. Guo, "Spreading of partially coherent Hermite-Gaussian beams through a non-Kolmogorov turbulence," *Optik — International Journal for Light and Electron Optics*, Mar. 9, 2011.

32. Qiu, Y., H. Guo, and Z. Chen, "Paraxial propagation of partially coherent Hermite-Gauss beams," *Opt. Commun.*, Vol. 245, 21–26, 2005.
33. Shirai, T., A. Dogariu, and E. Wolf, "Mode analysis of spreading of partially coherent beams propagating through atmospheric turbulence," *J. Opt. Soc. Am. A*, Vol. 20, 1094–1102, 2003.
34. Laabs, H., "Propagation of Hermite-Gaussian-beams beyond the paraxial approximation," *Optics Commun.*, Vol. 147, 1–4, 1998.
35. Ji, X., X. Chen, and B. Lü, "Spreading and directionality of partially coherent Hermite-Gaussian beams propagating through atmospheric turbulence," *J. Opt. Soc. Am. A*, Vol. 25, 21–28, 2008.
36. Wu, Z.-S., H.-Y. Wei, R.-K. Yang, and L.-X. Guo, "Study on scintillation considering inner- and outer-scales for laser beam propagation on the slant path through the atmospheric turbulence," *Progress In Electromagnetics Research*, Vol. 80, 277–293, 2008.